Hindawi
Advances in Materials Science and Engineering
Volume 2023, Article ID 1970245, 15 pages
https://doi.org/10.1155/2023/1970245

Research Article

Properties and Application of Chemical Grouting Materials for Construction Joint Leakage

Baozhi Li,[1] Weiwei Han,[2] Shuyin Wu,[2] Yanyan Shi,[3] Pan Wang,[4] and Xiaoguo Wang[2]

[1]*CCCC Third Navigation Engineering Bureau Co., Ltd. Third Engineering Co., Ltd., Nanjing 210011, China*
[2]*Shandong University of Science and Technology, Qingdao 266590, China*
[3]*Qingdao Engineering Vocational College, Qingdao 266112, China*
[4]*Qingdao Geological Exploration Institute of China Metallurgical Geology Bureau, Qingdao 266109, China*

Correspondence should be addressed to Weiwei Han; 258204143@qq.com

Received 17 August 2022; Revised 1 October 2022; Accepted 2 November 2023; Published 22 November 2023

Academic Editor: Minghui Gong

This paper aims to disclose the properties of the chemical grouting materials under different conditions. Firstly, the water-soluble polyurethane (WPU) slurry, oil-soluble polyurethane (OPU) slurry, epoxy resin (EP) slurry, a slurry mixed by WPU slurry, and OPU slurry marked as (WPU + OPU) slurry were selected to test the properties. The setting time, volume shrinkage, and adhesive strength were measured under room conditions and water conditions. Then, the tunnel construction joints were simulated, and the injectability and water blocking effect were analyzed to evaluate the suitability of the different grouting slurry. In addition, the results were applied in the water leakage management of the Taihu Lake tunnel project. The test results showed that each of the four materials had its performance advantages and disadvantages and provided vital guidance for the engineering application.

1. Introduction

With the rapid development of the national economy and the implementation of strong transportation as an essential means of transportation infrastructure construction, the number and mileage continue to increase [1, 2]. Although China has technology and experience in underground engineering and tunnel construction, many tunnels have a different degree of water leakage during construction and operation due to the constraints of geological conditions [1, 3]. The groundwater will corrode the lining concrete, corrode the steel bars, cause structural deterioration, and reduce the service life, which is a severe threat to the operation stability and safety of the tunnel [4, 5].

According to the water leakage survey, combined with the tunnel geological environment [6], construction level, material characteristics [7], and structural form [8], the management of the water leakage problems required a comprehensive analysis to grasp the causes of leakage, the consideration of the technical feasibility and economical type, the choice of the appropriate methods, materials, and construction technology to improve the efficiency and ensure the management effect. The grouting method was the most commonly used in water leakage management due to its simple process and strong adaptability to the complex environment [9, 10]. Meanwhile, the grouting method played the effect of water blocking and reinforcement, resulting in remarkable management [9, 11, 12].

The effect was closely related to the properties of the grouting materials. Compared to inorganic cement grouting slurry, the chemical grouting slurry had better injectability and was quicker to work, so they were often used in tunnel cracks, construction joints, and other small fracture openings. The polyurethane was the product of the polymerization reaction between the isocyanate and polyols [13, 14], and the response could also provide the expansion force to fill the cracks, voids, or fracture, with the characteristics of high expansion [15], permeability, durability [16], and fast solidification [17, 18]. The epoxy resin had outstanding potential as a grouting material [19], as it possessed superior strength [20], sufficient adhesive strength [21], and low

shrinkage [22]. Meanwhile, the epoxy resin was easy to be prepared as tunable formulations [19]. Acrylate grouting material was a highly elastic gel formed by acrylate monomers as the main agent, water as a diluent, and under certain initiators and promoters [23, 24]. The materials had a greater advantage: low viscosity, high permeability, and aging resistance. Meanwhile, it should be pointed out that the acrylate grouting material was prohibited in areas where they need the reinforcing effect [23].

However, there were diverse chemical grouting slurries with various properties. The commonly used slurries vary considerably in their treatment effectiveness, leading to a certain degree of empiricism in selecting the grouting slurries. In this study, four different chemical slurries were analyzed: WPU slurry, OPU slurry, EP slurry, and the slurry mixed by WPU slurry and OPU marked as (WPU + OPU) slurry. The setting time, volume shrinkage, and adhesive properties were measured under different conditions. The tunnel construction joints were simulated, and the injectability and water blocking effects were analyzed to evaluate the suitability of the various grouting slurry. In addition, the results were applied in the water leakage management of the Taihu Lake tunnel project.

2. Experiments and Methods

2.1. Material. Water-soluble polyurethane (WPU) and oil-soluble polyurethane (OPU) were purchased by the Shanghai Zhenmu Waterproofing Materials Institute, and their properties are shown in Table 1. Epoxy resin (EP) was provided by the Nanjing Ruidi High-Tech Institute, and the properties are shown in Table 2.

ASTM Type I PC from Shanshui Cement Plant in Jinan, China, was used in this study. The density was 3.01 g/cm^3, and the specific surface area was 332 m^2/kg. The fine aggregate was medium sand, and the fineness modulus was 2.6. The coarse aggregate was a continuous gradation range from 5 to 25 mm. Class F fly ash and mineral powder were used in this study. The fineness of fly ash was 43 μm, and the density was 2.4 g/cm^3, while the specific surface area of mineral powder was 414 m^2/kg, and the density was 2.88 g/cm^3. The superplasticizer provided by Shanhai Chemical Technology Institute and topwater from Qingdao was selected.

2.2. Test Programs

2.2.1. Setting Time. The setting time of the grouting slurry was the critical parameter in the grouting process and affected the spread of the slurry and the water blocking effect [25]. For OPU, the setting time tests were measured by adding 20 g of materials to 100 g of water according to JC/T 2041-2010. The solution was stirred thoroughly and left to stand until the wire drawing appeared between the glass rod's surface. The test method of WPU was similar to OPU, except the mass of water was 4 g due to its characteristic of water swelling. For EP, the setting time was measured by the A and B solution's viscosity exceeding 200 MPas after mixing.

2.2.2. Shrinkage. The water-soluble grouting material would have a considerable volume shrinkage after the water loss, resulting in a negative effect on the water blocking effect [26]. So, only the WPU and (WPU + OPU) were selected to measure the volume shrinkage. Two curing conditions were set: room curing condition and water curing condition. Then, three specimens were set to reduce errors. The WPU grouting material was mixed with 20 g WPU and 4 g water. The (WPU + OPU) grouting material was mixed with 20 g WPU, 20 g OPU, and 20 g water. The specimens are shown in Figure 1.

The volume shrinkage of the specimens was measured at 1 h, 6 h, 12 h, 1 d, 3 d, 5 d, 7 d, 14 d, and 21 d. The shrinkage was conducted to an indirect method. The anhydrous alcohol was poured into a 500 ml beaker until the balance showed a mass of 717.6 g when it was considered to be complete. The specimens were placed softly into the beaker, and the mass of the drained alcohol was measured. Then, the volume of the specimens was calculated by the drained mass and the density. The volume shrinkage rate was measured by the following equation:

$$\Delta k = \frac{v_0 - v_n}{v_n} \times 100\%, \quad (1)$$

where Δk is the volume shrinkage rate, %; v_0 is the initial volume of the specimens, ml; and v_n is the volume at the test time.

2.2.3. Adhesive Property. After solidification, the slurry needs to exhibit an excellent adhesive property with concrete to seal the water leakage. The tensile strength was calculated to measure the adhesive property. The WD-P6205 universal testing machine was used to measure the tensile strength, and the loading speed was 100 N/s. The displacement described the deformability at fracture.

The cement mortar was prepared by the cement : sand : water = 1 : 3 : 0.5, and the size was 40 mm × 40 mm × 40 mm. Meanwhile, the stainless steel pipe was preburied to measure the tensile test when the mortar was poured. The two specimens were placed in a flat position, with the side without the steel pipe placed opposite each other, and the Vernier caliper was used to determine the distance (5 mm). The tape was used to wrap the two specimens around the fracture, and the grouting opening was left. Then, the slurry was injected into the fracture, and the tape was removed after solidification. As shown in Figure 2, the WPU and (WPU + OPU) were cured under room and water conditions for 7 d, while the OPU and EP were only placed in the room.

2.2.4. Injectability. The injectability of the slurry was directly related to the water blocking effect and was measured by the simulation test. The design of the concrete is shown in Table 3. In order to simulate the actual construction process of horizontal construction joints, the test concrete was poured in four steps, as shown in Figure 3.

(1) Concrete was mixed according to the design, and the height was 75 mm (first pouring concrete). Then, it

Table 1: The properties of OPU and WPU.

	Density (g/cm^3)	Viscosity (MPa·s)	Setting time (s)	Nonvolatile content (%)	Foaming rate (%)	Compressive strength (MPa)	Water swelling rate (%)
OPU	1.204	2200	433	89	2943	24	
WPU	1.12	880	21	88	532		31

Table 2: The properties of EP.

	Density (g/cm^3)	Viscosity (MPa·s)	Setting time (s)	Compressive strength (MPa)	Tensile strength (MPa)	Adhesive strength (MPa)
EP	1.096	85	2100	85	15.8	63

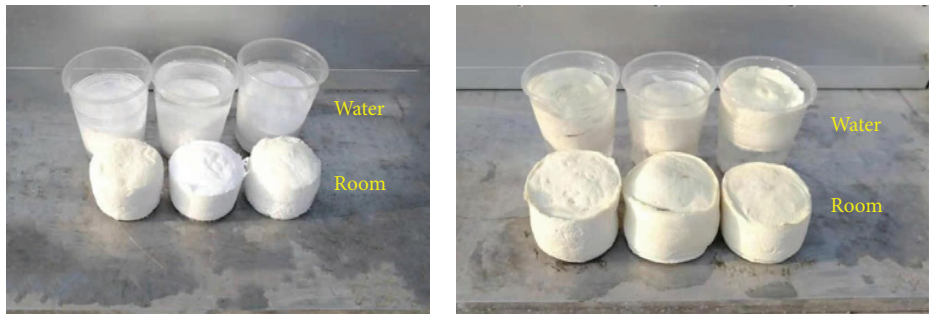

(a) (b)

Figure 1: The specimens of volume shrinkage: (a) WPU and (b) (WPU + OPU).

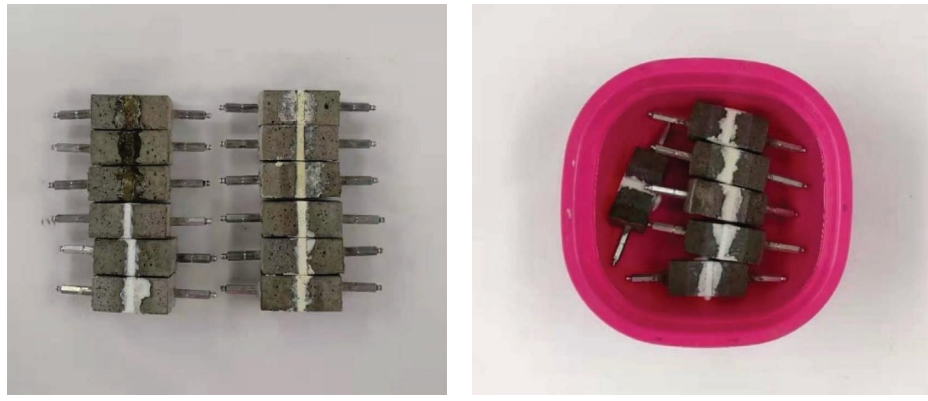

(a) (b)

Figure 2: The adhesive specimens under different curing conditions: (a) room and (b) water.

was thoroughly vibrated and compacted and cured at temperature for 48 h after removing the mold for 3 d further curing;

(2) An electric hammer was used for precise chiseling to remove the floating slurry on the surface of the concrete, and coarse aggregate was exposed on the interface until the coarse aggregate area on the surface of the concrete reached 50%;

(3) The scum and dust were removed, and the cement-based permeable crystalline waterproof coating was brushed;

(4) The concrete was continued to pour until the height was 75 mm (postpouring concrete) and cured at temperature for 48 h after removing the mold for 3 d further curing.

The key to injectability test was to ensure the interface sealing between mold and test sample. The modified epoxy resin is used to seal the samples, as shown in Figure 4. After the epoxy resin is solidified, the water pressure is added to check the tightness of the test block. If the water seepage point occurs, the modified acrylic resin is used for reinforcement.

The grouting pressure was set as 0.4 MPa, 0.8 MPa, and 1.2 MPa. A hole was drilled vertically at the center of the specimens using an electric hammer to a depth of 80 mm. Then, the injectability test was carried out after installing water stop pins.

2.2.5. Water Blocking Effect. The control of the water leakage was the most critical indicator for evaluating the suitability of the grouting materials. The preparation and sealing of the specimens were similar to those mentioned in Section 2.2.4. The test device was designed and fabricated in the laboratory. As shown in Figure 5, the test device was composed of a pneumatic loading part, a hydraulic loading part, a data acquisition part, and an assembled tank for the specimens. Based on the cumulative flow of the water leakage, the

Table 3: Experimental design of test concrete.

Cement	Fine aggregate	Coarse aggregate	Fly ash	Mineral powder	Water	Superplasticizer
218	753	1083	110	40	144	4

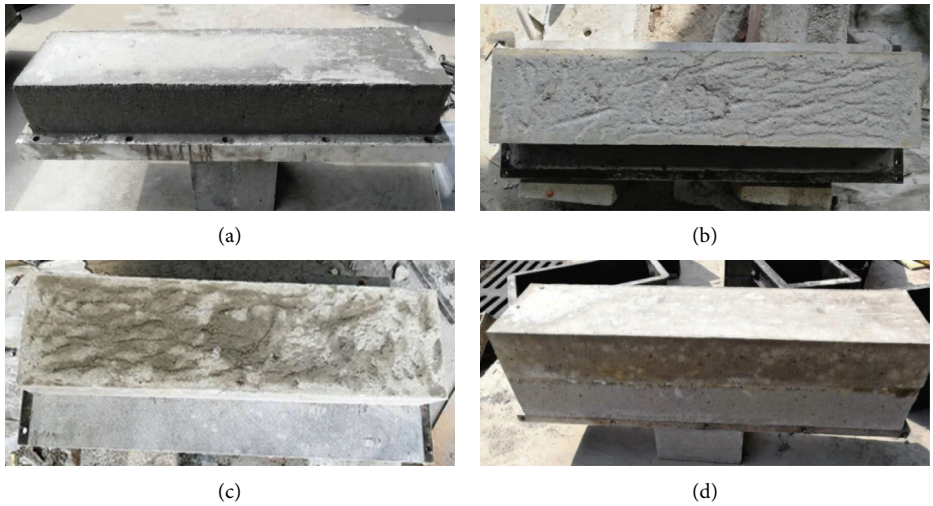

Figure 3: Pouring of concrete.

Figure 4: Sample sealing.

specimens were divided into three grades, as shown in Table 4. Furthermore, the pressure of the grouting slurry was set as 0.4 MPa to avoid ineffective diffusion.

3. Results

3.1. Setting Time. As shown in Table 5, the experimental setting times of the slurry were all larger than those of the standard condition (Tables 1 and 2). Therefore, the field experiments should be carried out before the grouting to determine the ideal setting time and the end criteria.

3.2. Volume Shrinkage. From Table 6, it can be found that the curing condition had a significant influence on the volume change of the slurry. Volume shrinkage occurred in the room condition, while the volume of the specimens was expanded in the water condition due to the water absorption effect. In addition, the WPU had a significant water loss and shrinkage properties compared to the (WPU + OPU) in the water condition. This was attributed to the excellent hydrophilicity and elasticity of WPU and the severe volume expansion compared to OPU. This caused a large volume shrinkage after water loss and correspondingly a larger volume shrinkage than (WPU + OPU).

In order to accurately describe the volume shrinkage process of the specimens, the volume shrinkage rate was plotted according to the test results for different periods, and the results are shown in Figure 6. It can be found that the development of volume shrinkage in room curing conditions was similar for both slurries and the rate of volume shrinkage was faster in the initial stage and then decreased gradually. The volume of the WPU slurry reached stability at around 15 d, while the (WPU + OPU) slurry reached stability at about 7 d.

The whole process of the water loss and shrinkage of the slurry can be divided into three stages: rapid shrinkage, deceleration shrinkage, and stabilization. The slurry's water loss and shrinkage process was the process of both internal water diffusion and surface water vaporization. The rapid shrinkage stage was the process of water migration from the periphery of the slurry and vaporization on the surface of the specimen. The deceleration shrinkage stage was the material internal moisture migration outward and in the test piece surface vaporization process. The water transport path increased at this time, and the water loss process development became slower. In the final, the water loss process was basically finished, and the volume of the materials was stable.

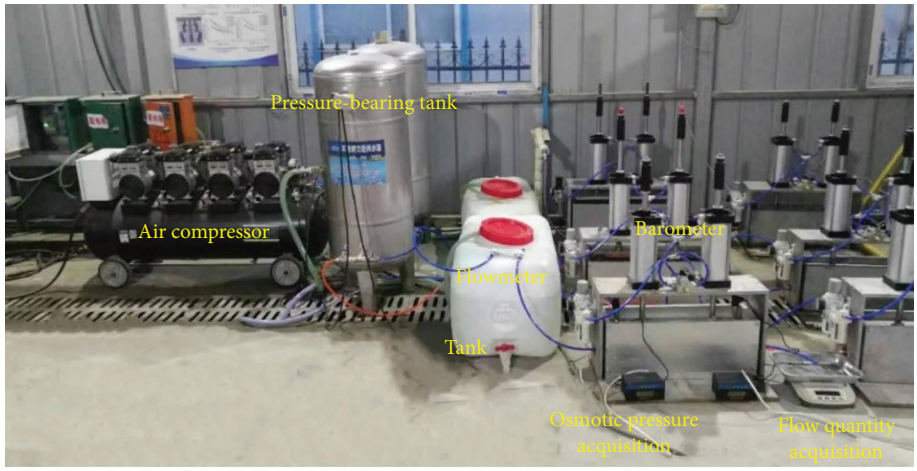

Figure 5: Test device.

Table 4: Water leakage grade evaluation.

Grade	Cumulative flow	Characteristics
S_I	0–10 mm^3/s	Wet
S_{II}	10 mm^3/s–60 mm^3/s	Slow leakage
S_{III}	>60 mm^3/s	Rapid leakage

Table 5: Setting time of different materials.

Grouting material	WPU	OPU	EP
Experimental setting time (s)	43.3	462.3	2370
Standard setting time (s)	21	433	2100

Table 6: Volume shrinkage rate of the materials under different curing conditions.

Grouting material	WPU		(WPU + OPU)	
Curing condition	Room	Water	Room	Water
Volume shrinkage rate (%)	82.77	−10.51	33.49	−2.06

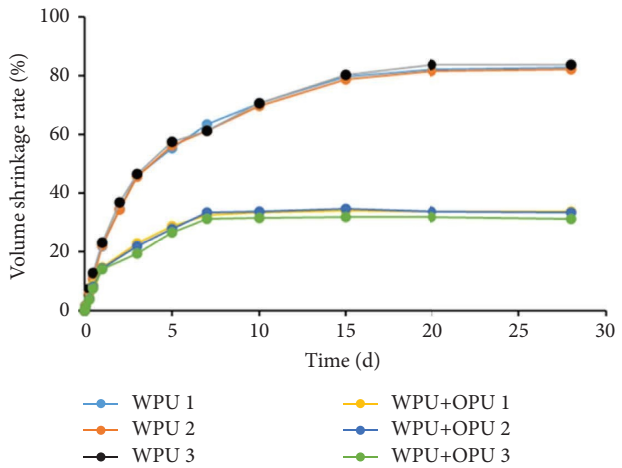

Figure 6: Volume shrinkage process of slurry in the room environment.

The WPU grouting slurry was unsuitable when the area had high water content in terms of material water loss and shrinkage characteristics. It was attributed that the WPU was easy to detach from the concrete surface, resulting in the potential and repeated water leakage problems.

3.3. Adhesive Property

3.3.1. Adhesive Interface. The damage in the interface can reflect the bonding ability of the slurry to the concrete. The damaged state of the specimens can be divided into three parts due to the location: interface, grouting materials, and concrete. As shown in Figures 7 and 8, the damage location of OPU and (OPU + WPU) was in the materials, while the WPU was in the interface and the EP was in the concrete, separately.

3.3.2. Deformability. The displacements at breakage of the materials were counted, and the elongations were concluded to reflect the deformation capacity. As shown in Table 7, the deformation characteristic of the materials under various curing conditions differed due to their properties, and the order was WPU (water) > WPU (room) > (WPU + OPU) (water) > (WPU + OPU) (room) > OPU > EP. The WPU slurry formed an elastomer after solidification and could produce large deformation, while the OPU slurry and EP slurry would include hard solid with poor deformation properties. In addition, the (WPU + OPU) slurry combined the characteristics of both parts to show intermediate performance. The deformation capacity of the WPU and (WPU + OPU) varied under different curing conditions because the WPU slurry lost water and shrank in the air, and the ability to inhibit deformability was decreased.

3.3.3. Adhesive Strength. As shown in Table 8, similar to the deformation capacity, the adhesive strength also differed under various curing condition and material types, and the order was EP > (OPU + WPU) (room) > (OPU + WPU)

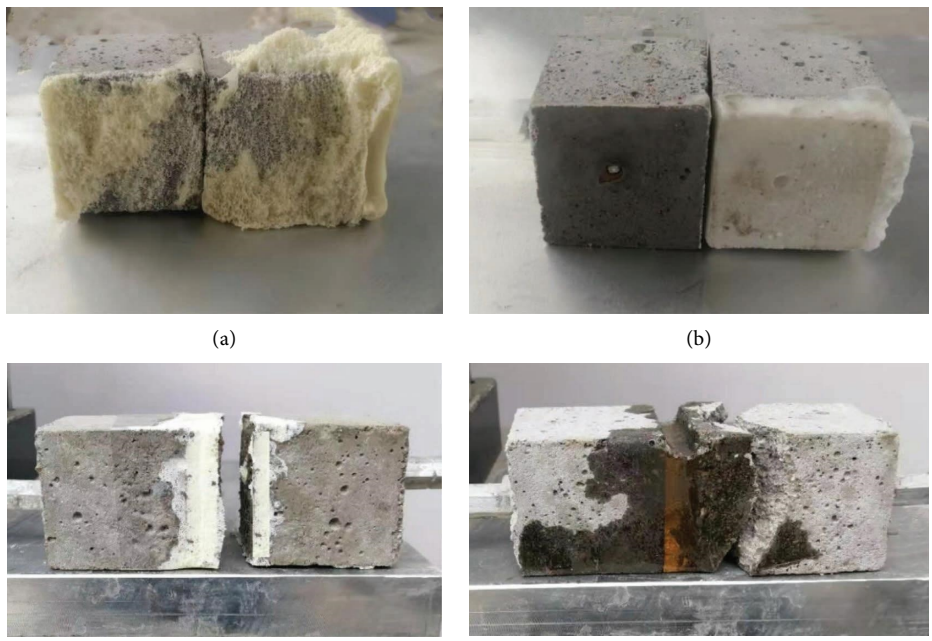

(a) (b) (c) (d)

Figure 7: The damage state under room curing conditions. (a) OPU, (b) WPU, (c) (OPU + WPU), and (d) EP.

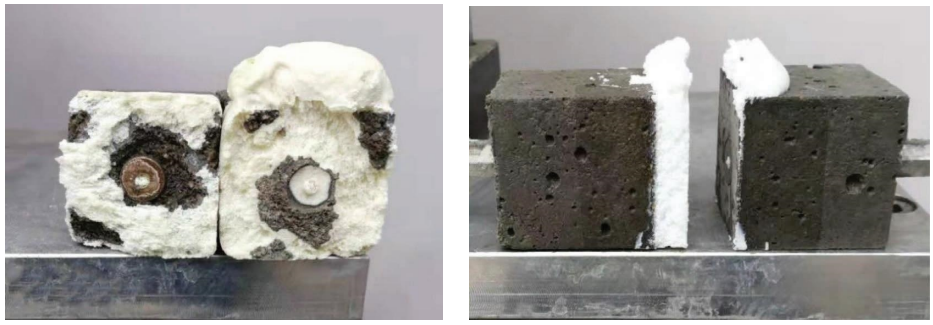

(a) (b)

Figure 8: The damage state under water curing conditions. (a) (OPU + WPU) and (b) WPU.

Table 7: Displacement value of the materials under different curing conditions.

Curing condition	WPU Room	WPU Water	(WPU + OPU) Room	(WPU + OPU) Water	OPU Room	EP Room
Displacement (mm)	2.83	3.47	2.33	2.43	0.3	0.21
Elongation (%)	56.6	69.4	46.6	48.6	6	4.2

(water) > WPU (room) > WPU (water) > OPU. The adhesive strength of the WPU material was strongly influenced under the different curing conditions, and the strength under room conditions was 2.2 times higher than that under water conditions, while for (WPU + OPU) material, the difference was not significant.

Combined with the above analysis, it can be observed that the OPU grouting slurry should not be applied in the area with large deformation. Although the OPU grouting material had a specific adhesive strength, its deformation capacity was poor. The WPU grouting slurry was not suitable when the reinforcement was required, for it was elastic after solidification and had poor reinforcement capacity. Compared to the traditional cement material, the chemical slurry was easy to cause damage and formed the new water leakage channels due to its low strength. This is the reason for the poor durability of chemical slurries.

3.4. Injectability

3.4.1. Slurry Dispersion Distance. As shown in Figure 9, it was observed that the diffusion distances of the four grouting

Table 8: Adhesive strength of the materials under different curing conditions.

Curing condition	WPU Room	WPU Water	(WPU + OPU) Room	(WPU + OPU) Water	OPU Room	EP Room
Adhesive strength (kPa)	174	79	297	296	76	647

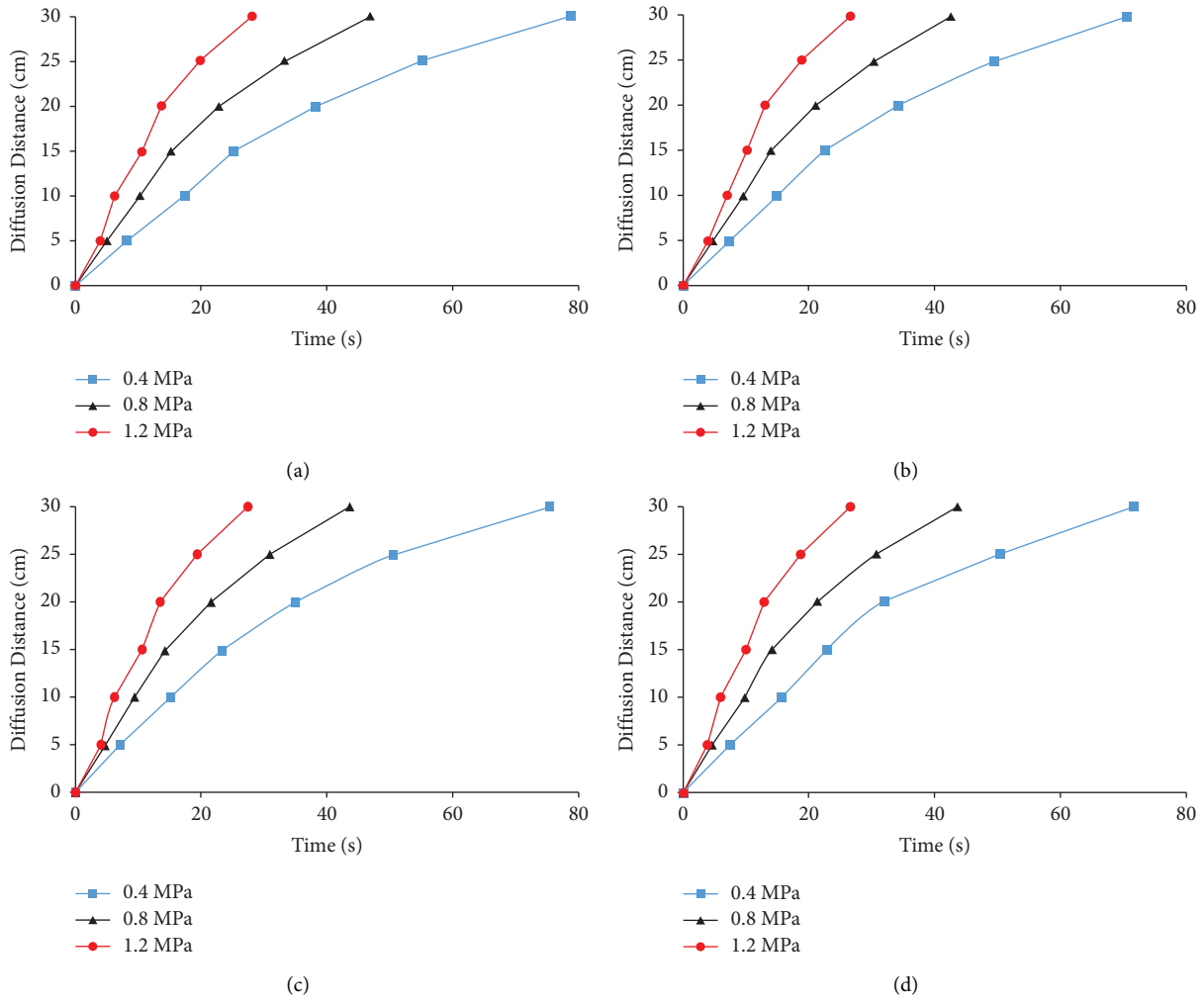

Figure 9: Relationship between the slurry diffusion distance and time. (a) OPU slurry, (b) WPU slurry, (c) (WPU + OPU) slurry, and (d) EP slurry.

slurries varied in a similar pattern with time, and the distance increased with the grouting time. At the same grouting pressure, the slurry diffused faster at the beginning, and the diffusion rate gradually decreased. As the grouting pressure increased, the time for the slurry to diffuse to the fracture decreased. For example, the time for OPU slurry at 0.4 MPa was 78.6 s, while 46.8 s and 28 s for 0.8 MPa and 1.2 MPa, respectively. The diffusion time of the four grouting slurries to the fracture under the same pressure was similar. For the 0.4 MPa pressure, the time of the OPU slurry was 78.6 s, the WPU slurry was 70.8 s, the (WPU + OPU) slurry was 75.6 s, and the EP slurry was 70.5 s.

Considering the thickness of tunnel lining was generally small in practice, if the grouting pressure was high, the slurry would be transported to the fracture in a relatively short time. If the slurry time was too long and solidification could not occur during the grouting process, the slurry would be washed out of the fracture under the influence of grouting pressure, resulting in a low retention rate and poor grouting blocking effect. Therefore, the grouting pressure was suitable for 0.4 MPa.

3.4.2. Pressure. As shown in Figure 10, the spatial and temporal distribution of grouting pressure was similar for all four grouting slurries, and the pressure decreased with the increased diffusion distance. It was attributed that the slurry was affected by the frictional resistance of the fracture wall and its viscosity during the diffusion process, so the grouting pressure tended to decay. The decline of the pressure, as the

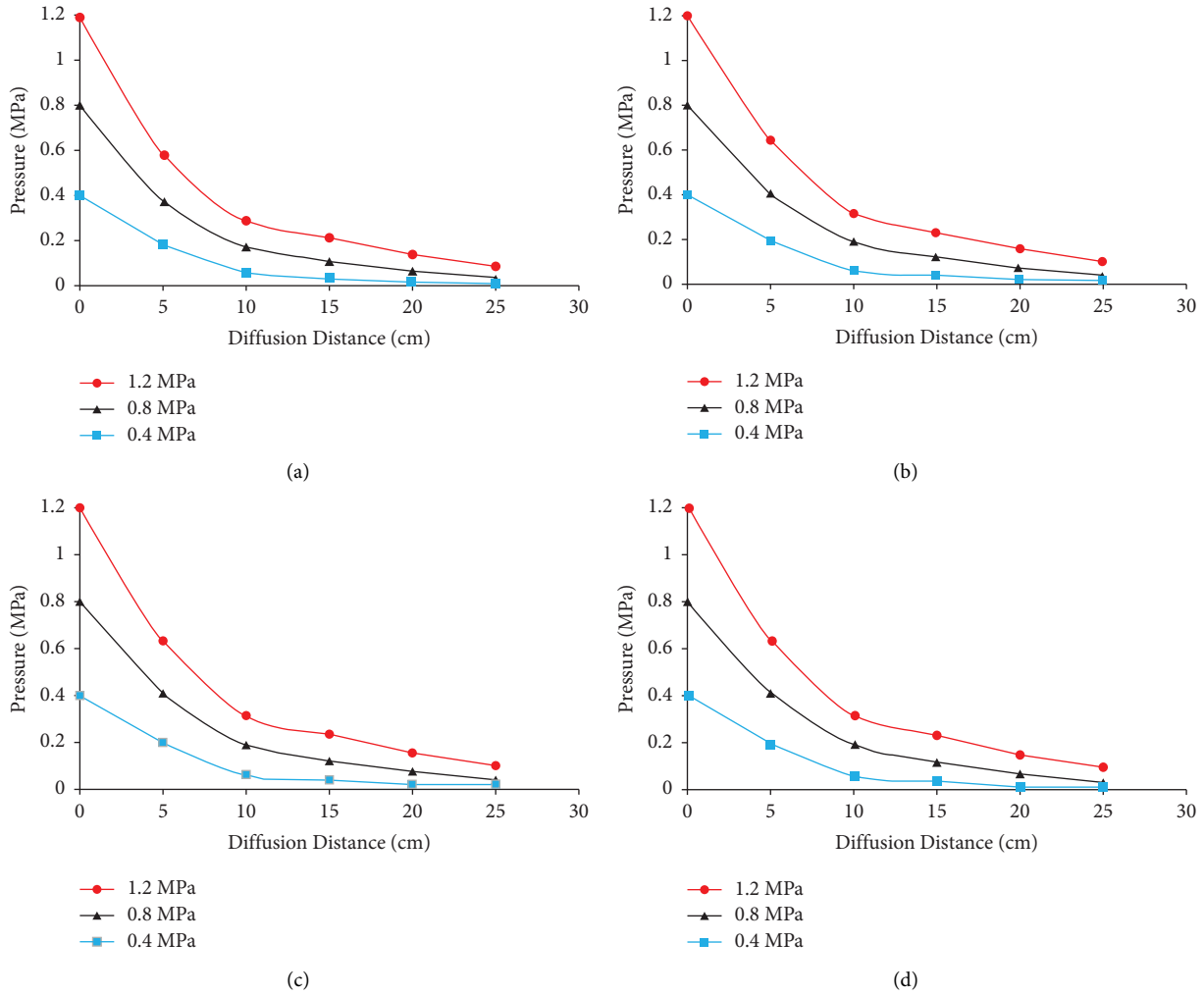

Figure 10: Relationship between the pressure and slurry diffusion distance. (a) OPU slurry, (b) WPU slurry, (c) (WPU + OPU) slurry, and (d) EP slurry.

driving force, was closely related to the rate of slurry transport, with the overall declined pressure being rapid at the early grouting time, followed by a gradual decrease in the reduced rate of the grouting pressure.

3.5. Water Blocking Effect. Based on the relationship between the flow and time in Figures 11–13, the curves could be divided into three types: single-platform decrease, multiplatform decrease, and multiplatform stability. The single-platform decreasing type and multiplatform decreasing type were both able to seal the water leakage. In comparison, the multiplatform stable type failed to seal the leakage.

The single-platform decreasing type could be divided into four parts:

(1) The initial stabilization stage: The water flowed along the seepage path under water pressure, and the seepage volume was in a stable stage.

(2) The rapid growth stage: The slurry entered the fracture under the grouting pressure. The slurry had not solidified, and the slurry drove the water into the fracture at this time. The seepage velocity increased significantly, and the initial smooth stage was broken, so the flow rate increased rapidly and reached the peak of dynamic water flow rate in a short time.

(3) The stable seepage stage: The grouting time continued to increase, and the slurry had not reached the setting time. The water and slurry cotransportation state in the fracture remained stable, so the flow rate was also regular.

(4) The fast decline stage: The slurry gradually reached the setting time with the increase of time, and the initial grouting slurry diffusion to the edge of the fracture after solidification. The slurry bonded to the fracture wall, and the flow rate decreased. As the later grouting slurry further solidified, the fracture was completely sealed by the slurry, so the amount of seepage was 0 at that time.

The multiplatform decreasing type could be divided into five parts:

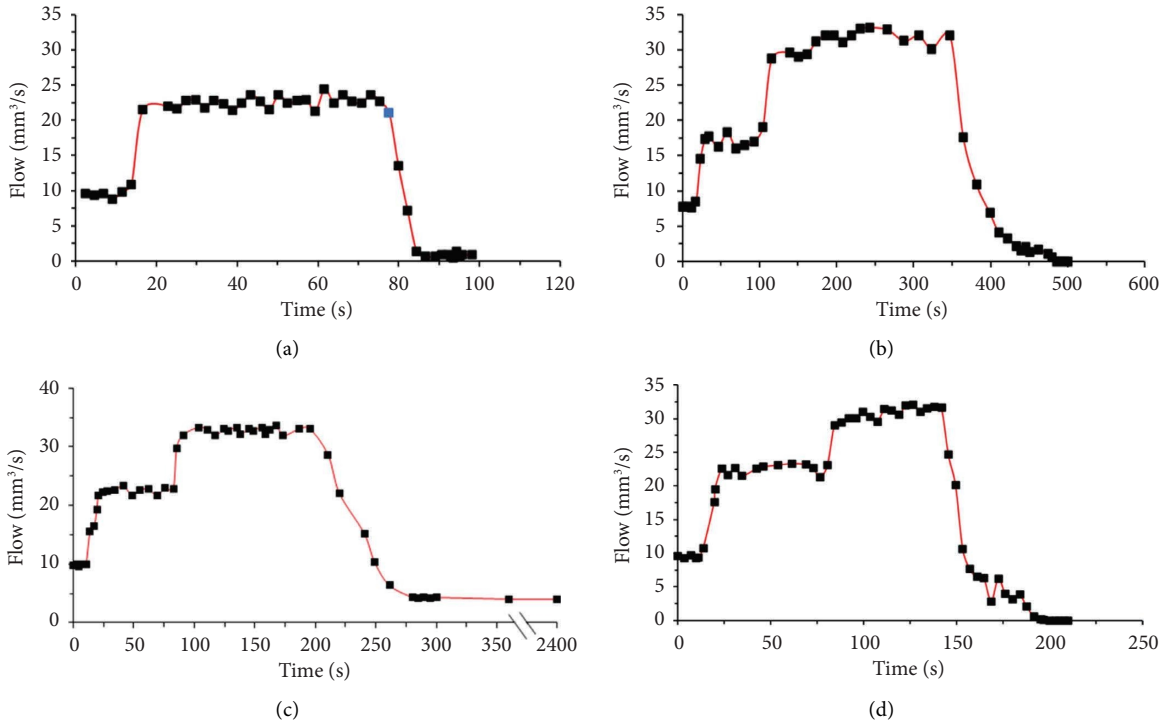

Figure 11: Relationship between the flow and time under grade S_I. (a) WPU slurry, (b) OPU slurry, (c) EP slurry, and (d) (WPU + OPU) slurry.

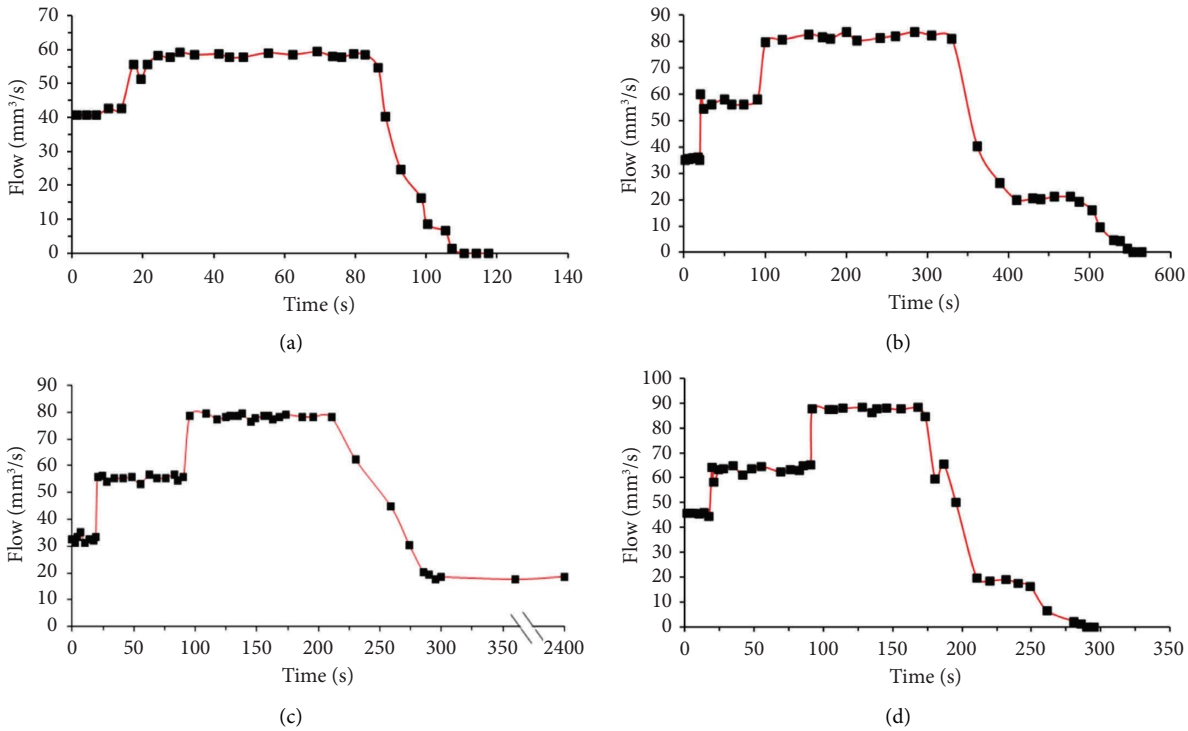

Figure 12: Relationship between the flow and time under grade S_{II}. (a) WPU slurry, (b) OPU slurry, (c) EP slurry, and (d) (WPU + OPU) slurry.

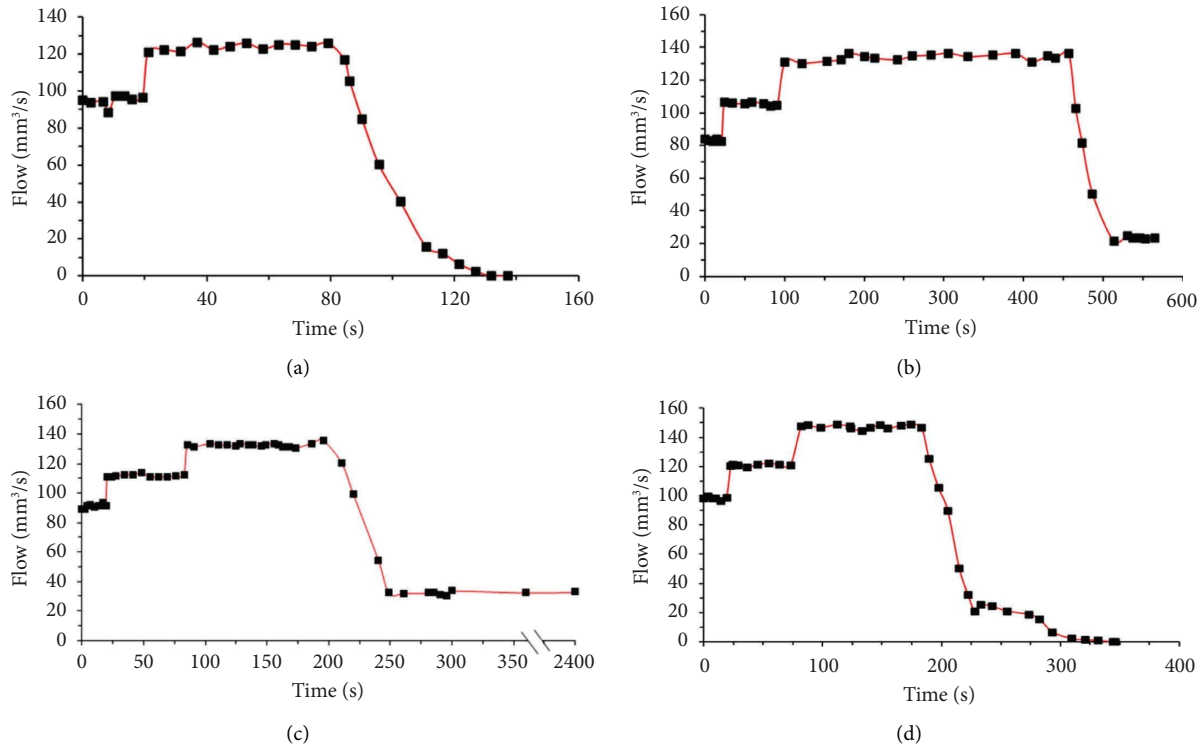

FIGURE 13: Relationship between the flow and time under grade S_{III}. (a) WPU slurry, (b) OPU slurry, (c) EP slurry, and (d) (WPU + OPU) slurry.

(1) The initial stabilization stage.

(2) The rapid growth stage.

(3) The first stable seepage stage: The state of water and slurry cotransportation in the fracture remained stable, so the flow rate was also regular.

(4) The second stable seepage stage: The fracture was still transported by both slurry and water together and remained in a steady state. As the grouting time increased, the slurry gradually spread to the fracture edge, and the outlet flow rate grew rapidly and then remained stable.

(5) The gradual decline stage: At the end of the grouting process, the flow rate of the outlet was reduced, and the grouting slurry gradually solidified and formed a certain bond strength with the concrete so that the water leakage channel was reduced and the water leakage flow rate of the fracture was lower. With the complete gradual curing of the slurry, all the water leakage channels were sealed, and the water seepage at the outlet was gradually reduced to 0.

The multiplatform stable type could be divided into five parts:

(1) The initial stabilization stage.

(2) The rapid growth stage.

(3) The first stable seepage stage.

(4) The second stable seepage stage.

(5) The third stable seepage stage: At this stage, the flow rate was lower than the initial time, and complete sealing was not achieved. At the end of the grouting process, the flow rate of the outlet was reduced, and the grouting slurry gradually solidified and formed a certain adhesive strength with the concrete so that the water leakage channel was reduced and the water leakage flow rate of the fracture was lower. However, due to the long setting time of the slurry, the leakage water flow was larger, the slurry failed to seal the remaining leakage water channels during the process of complete gelation, the outlet flow was again in a stable stage, and the blocking failed.

As shown in Figure 11, it was observed that the WPU, OPU, and (WPU + OPU) slurries could achieve the water leakage sealing. The WPU and OPU slurries were single-platform decreasing types, the (WPU + OPU) slurry was multiplatform decreasing types, and EP slurry was the multiplatform stable type. The slurry was flushed out of the fracture under the grouting pressure due to the long setting time, and the slurry did not react chemically with the water. After the grouting process was finished, some slurries would remain in the fracture. At the same time, the leakage water flow was small, and the slurry viscosity was large. The slurry would remain in the fracture. Then, the water leakage channels were formed in the middle of the slurry, and the stable flow rate was formed after the solidified slurry. In addition, the flow

Table 9: Water blocking effect of different levels of water leakage.

Water leakage grade	Grouting slurry	Flow curve type	Water blocking
S_I	WPU	Single-platform decreasing type	Yes
S_I	OPU	Multiplatform decreasing type	Yes
S_I	EP	Multiplatform stable type	No
S_I	(WPU + OPU)	Multiplatform decreasing type	Yes
S_{II}	WPU	Single-platform decreasing type	Yes
S_{II}	OPU	Multiplatform decreasing type	Yes
S_{II}	EP	Multiplatform stable type	No
S_{II}	(WPU + OPU)	Multiplatform decreasing type	Yes
S_{III}	WPU	Single-platform decreasing type	Yes
S_{III}	OPU	Multiplatform stable type	No
S_{III}	EP	Multiplatform stable type	No
S_{III}	(WPU + OPU)	Multiplatform decreasing type	Yes

rate was reduced from the initial value, and the degree depended on the amount of the slurry that remained.

It was found that the WPU slurry, OPU slurry, and (WPU + OPU) slurry could seal the water leakage. The EP slurry failed to achieve the water leakage sealing, and it was the multiplatform stable type, with a reduction in dynamic water flow compared to the initial value after solidification.

As shown in Figure 13, the WPU slurry and (WPU + OPU) slurry could seal the water leakage. WPU slurry was a single-platform decreasing type, while the (WPU + OPU) slurry was a multiplatform decreasing type. The OPU slurry and EP slurry could not achieve the water leakage sealing, and all belonged to the multiplatform stable type. Additionally, the water blocking results are summarized in Table 9.

4. Discussion

The sealing of water leakage was summarized to analyze the suitability of the current chemical grouting slurries commonly used in construction joints to the volume shrinkage and the adhesive properties with the concrete, and the result is shown in Table 10.

WPU grouting slurry had good water blocking effect at different water leakage levels. However, its solidification had prominent volume shrinkage characteristics in air, resulting in poor durability and repeated water leakage. When immersed in water, the volume of the WPU slurry absorbed water and expanded, significantly reducing the probability of repeated leakage. The WPU slurry had low adhesive strength and specific deformation capacity, suitable for the environment with little water content.

OPU grouting slurry was capable of sealing water leakage at S_I and S_{II}, and failed at S_{III}. The slurry after solidification had no volume shrinkage and had a low adhesive property to the concrete, making it suitable for the management without dynamic water and required reinforcement.

(WPU + OPU) slurry achieved water leakage sealing at all three levels. The slurry had a minor volume shrinkage and excellent adhesive strength. So it could be applied to water leakage management problems where the dynamic water conditions require reinforcement.

EP grouting slurry failed to seal water leakage at any status. The slurry after solidification had no volume shrinkage and had a high adhesive strength to the concrete, making it suitable for water leakage management in a water-free environment and where the reinforcement was required. WPU grouting slurry could be applied first to achieve water leakage sealing in the area containing water. Then, EP grouting was used to solve the problem of the lack of durability of WPU grouting slurry. Similarly, the applicability of EP slurry was also solved.

5. Engineering Application

Taihu Lake tunnel is a 10.79 km long project under construction. Due to the need for the tunnel crossing the bottom the Taihu Lake, water leakage diseases often occur during the construction process under the sufficient water supply. Based on the project, a slurry blocking and reinforcement solution was designed for the water leakage disease in the tunnel construction joints. The results in this study on the applicability of the grouting materials were used to ensure the long-term stability of the tunnel during operation.

Through the on-site investigation and statistics, it was found that there was more water leakage in the tunnel K24 + 000~K25 + 250. The construction joints were a high water leakage area, accounting for 69% of the total. The water leakage was mainly in the form of wet (S_I) and slow leakage (S_{II}), and few remains were the rapid leakage (S_{III}).

From the analysis of the water blocking effect, WPU slurry, OPU slurry, and (WPU + OPU) slurry could be selected when the water leakage grade was S_I and S_{II}, while the WPU slurry and (WPU + OPU) slurry could be chosen for the S_{III} grade. The change of groundwater in this project was not significant, so the volume shrinkage of the WPU slurry was not obvious. Meanwhile, the tunnel lining thickness was 80 cm~140 cm, and the slurry diffusion path is short, so the initial recommended grouting pressure was 0.4 MPa, which would need to be optimally adjusted according to the situation in the actual field.

The commonly used borehole grouting method was adopted to manage the water leakage, and the main steps are shown in Figure 14. The water blocking effect after grouting

Table 10: Applicability analysis of grouting slurries for water leakage in construction joints of tunnel lining.

Grouting slurry	Blocking speed	Water blocking effect			Volume shrinkage		Adhesive strength		Injectability
		S_I	S_{II}	S_{III}	Water	Room	Water	Room	
WPU	Fast	Yes	Yes	Yes	Good	Average	Average	Average	Good
OPU	Average	Yes	Yes	No		None		Average	Good
(WPU + OPU)	Average	Yes	Yes	Yes	Good	Average	Good	Good	Good
EP	Slow	No	No	No		None		Good	Good

(a) (b) (c) (d)

Figure 14: On-site grouting operation process. (a) Borehole. (b) Stopper pins. (c) Slurry stirring. (d) Grouting operation.

Figure 15: Inspection of the partial grouting effect.

was observed and photographed, and the partial results are shown in Figure 15.

It can be found that after the management, the water blocking effect was significantly obvious. Before grouting, there was water leakage in the construction joints, and the surrounding area showed wet stains. Water leakage was not observed after the grouting effect, and the structure surface was completely dry after 72 h.

6. Conclusion

This study aims to declare the suitability of the current chemical grouting slurries (WPU slurry, OPU slurry, and EP slurry) commonly used in construction joints, and the results are shown as follows:

(1) The setting time of the slurry under test conditions differed from the standard conditions, indicating that the temperature had a significant effect on the setting time. So the test should be conducted in real time on-site during actual construction to determine the grouting parameters.

(2) WPU slurry and (WPU + OPU) slurry all had a volume shrinkage characteristic, and the varied pattern was similar. The initial volume shrinkage rate was fast and then slowed down with time. The volume shrinkage of WPU slurry was stable at 15 d, and the rate was 82.77% compared to the initial time, while the values were 28 d and 33.49% for (WPU + OPU) slurry.

(3) The order of the adhesive strength was WPU (water) > WPU (room) > (WPU + OPU) (water) > (WPU + OPU) (room) > OPU > EP, while the deformation capacity was WPU (water) > WPU (room) > (WPU + OPU) (water) > (WPU + OPU) (room) > OPU > EP. The adhesive strength of WPU and (WPU + OPU) under room curing conditions was greater than that under water conditions. For the deformation capacity, the WPU under water conditions was higher than room conditions, while the (WPU + OPU) was similar under two conditions.

(4) The grouting slurries had good injectability, and the slurry diffusion pattern was similar. The slurry diffusion rate was positively correlated with the grouting pressure. The higher the grouting pressure, the short the time for the slurry to diffuse to the fracture edge. As the thickness of the lining

influences the construction joint grouting, the grouting pressure was suitable to set as 0.4 MPa.

(5) The time flow curves of grouting slurries were described as three types: single-platform decreasing type, multiplatform decreasing type, and multiplatform stable type. The single-platform decreasing type and the multiplatform decreasing type were capable of sealing water leakage. The multiplatform stable type cannot seal water leakage. The WPU slurry and the (WPU + OPU) slurry were able to seal the water leakage at different water leakage levels, and the OPU slurry could be applied in S_I and S_{II}. In addition, the EP slurry did not achieve water leakage management under any conditions.

(6) This study was applied to the Taihu Lake tunnel, and the water blocking effect was significantly noticeable.

Data Availability

The data used in this study are available on request from the corresponding author.

Conflicts of Interest

The authors declare that they have no conflicts of interest.

Authors' Contributions

Baozhi Li conceptualized the study, proposed the methodology, performed formal analysis, and provided resources. Weiwei Han investigated the study, wrote the original draft, curated the data, and performed funding acquisition. Shuyin Wu wrote the original draft. Yanyan Shi investigated the study, curated the data, and reviewed and edited the article. Pan Wang supervised and validated the study and reviewed and edited the article. Xiaoguo Wang curated the data, reviewed and edited the article, and validated the study.

Acknowledgments

The work was supported by the Key R & D project of Shandong Province (grant no. 2019JZZY010427) and the Natural Science Foundation of Shandong Province (grant no. ZR2021QE250).

References

[1] Z. Xu, J. Chen, Y. Luo et al., "Geomechanical model test for mechanical properties and cracking features of Large-section tunnel lining under periodic temperature," *Tunnelling and Underground Space Technology*, vol. 123, Article ID 104319, 2022.

[2] S. Quanke, Z. Yongling, C. Yue et al., "Hong Kong Zhuhai Macao Bridge-Tunnel project immersed tunnel and artificial islands – from an Owners' perspective," *Tunnelling and Underground Space Technology*, vol. 121, Article ID 104308, 2022.

[3] Y. Xue, X. Cai, M. Shadabfar, H. Shao, and S. Zhang, "Deep learning-based automatic recognition of water leakage area in shield tunnel lining," *Tunnelling and Underground Space Technology*, vol. 104, Article ID 103524, 2020.

[4] Z. Shijie, Z. Guyi, L. Deming, W. Shuyi, S. fei, and W. Chao, "The crucial techniques of water leakage treatment in operating highway tunnel," *IOP Conference Series: Earth and Environmental Science*, vol. 525, no. 1, Article ID 012160, 2020.

[5] L. Yanan, Z. Qingsong, L. Rentai et al., "Research on comprehensive analysis method for leakage treatment of underground engineering lining," *IOP Conference Series: Earth and Environmental Science*, vol. 189, no. 2, Article ID 022051, 2018.

[6] Y. Suyama, M. Toida, and K. Yanagizawa, "Study of an optimization approach for a disposal tunnel layout, taking into account the geological environment with spatially heterogeneous characteristics," *Nuclear Engineering and Design*, vol. 239, no. 9, pp. 1693–1698, 2009.

[7] B. Zhang, B. Wang, Y. Zhong, X. Li, Y. Zhang, and S. Li, "Damage characteristics and microstructures of low-exothermic polymer grouting materials under F–T cycles," *Construction and Building Materials*, vol. 294, Article ID 123390, 2021.

[8] Z. Yu, H. Dai, and Z. Shi, "Structural form-finding of bending components in buildings by using parametric tools and principal stress lines," *Frontiers of Architectural Research*, vol. 11, no. 3, pp. 561–573, 2022.

[9] Z. Xu, D. Pan, S. Li, Y. Zhang, Z. Bu, and J. Liu, "A grouting simulation method for quick-setting slurry in karst conduit: the sequential flow and solidification method," *Journal of Rock Mechanics and Geotechnical Engineering*, vol. 14, no. 2, pp. 423–435, 2022.

[10] H. Yu, T. Xu, Y. Yuan et al., "Enhanced heat extraction for deep borehole heat exchanger through the jet grouting method using high thermal conductivity material," *Renewable Energy*, vol. 177, pp. 1102–1115, 2021.

[11] X. Xu, Z. Wu, H. Sun, L. Weng, Z. Chu, and Q. Liu, "An extended numerical manifold method for simulation of grouting reinforcement in deep rock tunnels," *Tunnelling and Underground Space Technology*, vol. 115, Article ID 104020, 2021.

[12] S. Li, P. Wang, C. Yuan et al., "Adaptability of polyurethane/water glass grouting reinforcement to subsea tunnels," *Construction and Building Materials*, vol. 311, Article ID 125354, 2021.

[13] M. Li, M. Du, F. Wang, B. Xue, C. Zhang, and H. Fang, "Study on the mechanical properties of polyurethane (PU) grouting material of different geometric sizes under uniaxial compression," *Construction and Building Materials*, vol. 259, Article ID 119797, 2020.

[14] M. M. Demir, I. Yilgor, E. Yilgor, and B. Erman, "Electrospinning of polyurethane fibers," *Polymer*, vol. 43, no. 11, pp. 3303–3309, 2002.

[15] G. Harikrishnan and D. V. Khakhar, "Effect of monomer temperature on foaming and properties of flexible polyurethane foams," *Journal of Applied Polymer Science*, vol. 105, no. 6, pp. 3439–3443, 2007.

[16] J. Chen, X. Yin, H. Wang, and Y. Ding, "Evaluation of durability and functional performance of porous polyurethane mixture in porous pavement," *Journal of Cleaner Production*, vol. 188, pp. 12–19, 2018.

[17] X. Li, Z. Gao, J. Gu, F. Zhao, and X. Bai, "Synthesis and characterisation of one-part ambient temperature curing polyurethane adhesives for wood bonding," *Pigment and Resin Technology*, vol. 33, no. 6, pp. 345–351, 2004.

[18] J. Wang, Q. Mei, L. Lin et al., "A comparison of the characteristics of polyurethane-based sealers including various

antimicrobial agents," *Royal Society of Chemistry Advances*, vol. 9, no. 13, pp. 7043–7056, 2019.

[19] Y. Zhang, H. Pang, D. Wei et al., "Preparation and characterization of chemical grouting derived from lignin epoxy resin," *European Polymer Journal*, vol. 118, pp. 290–305, 2019.

[20] C. Wang, Z. Fan, C. Li, H. Zhang, and X. Xiao, "Preparation and engineering properties of low-viscosity epoxy grouting materials modified with silicone for microcrack repair," *Construction and Building Materials*, vol. 290, Article ID 123270, 2021.

[21] W. Wang, W. Zhao, J. Zhang, and J. Zhou, "Epoxy-based grouting materials with super-low viscosities and improved toughness," *Construction and Building Materials*, vol. 267, Article ID 121104, 2021.

[22] Y. Fang, B. Ma, K. Wei, X. Wang, X. Kang, and F. Liu, "Performance of single-component epoxy resin for crack repair of asphalt pavement," *Construction and Building Materials*, vol. 304, Article ID 124625, 2021.

[23] T. C. Han, "Gel time of calcium acrylate grouting material," *Journal of Zhejiang University- Science*, vol. 5, no. 8, pp. 928–931, 2004.

[24] A. Cinar and N. Maerz, "An experimental study of chemical grouting materials for optimum mechanical performance," *Geo-Congress 2020: Foundations, Soil Improvement, and Erosion*, American Society of Civil Engineers, pp. 716–726, Reston, VA, USA, 2020.

[25] Q. Zhang, L. Zhang, R. Liu, S. Li, and Q. Zhang, "Grouting mechanism of quick setting slurry in rock fissure with consideration of viscosity variation with space," *Tunnelling and Underground Space Technology*, vol. 70, pp. 262–273, 2017.

[26] Z. Tian, X. Liu, Z. Zhang, K. Zhang, and X. Tang, "Potential using of water-soluble polymer latex modified greener road geopolymeric grouts: its preparation, characterization and mechanism," *Construction and Building Materials*, vol. 273, Article ID 121757, 2021.